

Adopting flexibility of the end-plate connections in steel moment frames

M. Ghassemieh^{*1}, M. Baei^{2a}, A. Kari^{3b}, A. Goudarzi^{1c} and D.F. Laefer^{2d}

¹ School of Civil Engineering, University of Tehran, Tehran, Iran

² Urban Modelling Group, School of Civil, Structural and Environmental Engineering,
University College Dublin, Dublin, Ireland

³ Engineering Department, Qom University of Technology, Qom, Iran

(Received April 14, 2014, Revised October 17, 2014, Accepted November 15, 2014)

Abstract. The majority of connections in moment resisting frames are considered as being fully-rigid. Consequently, the real behavior of the connection, which has some level of flexibility, is ignored. This may result in inaccurate predictions of structural response. This study investigates the influence of flexibility of the extended end-plate connections in the steel moment frames. This is done at two levels. First, the actual micro-behavior of extended end-plate moment connections is explored with respect to joint flexibility. Then, the macro-behavior of frames with end-plate moment connections is investigated using modal, nonlinear static pushover and incremental dynamic analyses. In all models, the P-Delta effects along with material and geometrical nonlinearities were included in the analyses. Results revealed considerable differences between the behavior of the structural frame with connections modeled as fully-rigid versus those when flexibility was incorporated, specifically difference occurred in the natural periods, strength, and maximum inter-story drift angle.

Keywords: extended end-plate moment connection; flexibility; modal analysis; pushover analysis; incremental dynamic analysis

1. Introduction

An end-plate moment connection consists of a beam, a column, an end-plate, and a number of bolts. The end-plate connections are classified as either extended or flush end-plate connections and each as being in either an unstiffened or stiffened arrangement, as illustrated in Figs. 1 and 2.

Many researchers have investigated the behavior of end-plate moment connections using the assumption of rigid joints behavior. Full-scale tests by Ghassemieh *et al.* (1983) investigated the behavior of stiffened extended end-plate connections with eight bolts. In their study, full-scale connections were tested and finite element method (FEM) of analyses were conducted and

*Corresponding author, Professor, E-mail: mghassem@ut.ac.ir

^a Ph.D. Researcher, E-mail: mahmoud.baei@ucdconnect.ie

^b Assistant Professor, E-mail: kari@qut.ac.ir

^c M.Sc. Graduate, E-mail: a.goudarzi@ut.ac.ir

^d Associate Professor, E-mail: debra.laefer@ucd.ie



Fig. 1 Extended end-plate moment connections



Fig. 2 Flush end-plate moment connections

compared. From the results of the analyses, prediction equations characterizing the connections behavior were developed. Subsequently, Murray and Kukreti (1988) simplified the design equations developed by Ghassemieh *et al.* (1983), which were adopted into the AISC Manual of Steel Construction (1989). Kukreti *et al.* (1990) compared the results of the extended, end-plate tests with the prediction equations developed from regression analyses of many end-plate cases. Their study resulted in more realistic equations for predicting the connection behavior with eight bolts in four rows. Popov and Tsai (1989) performed some experimental tests with cyclic loading on some moment connections in order to attain an ideal connection configuration. Results showed that an end-plate moment connection is a suitable replacement for a fully welded connection in seismic resistant frames. A year later, the same authors proposed that the methods used in static analyses should be revised for seismic loading for end-plate moment connection (Tsai and Popov 1990). Subsequently, Bahaari and Sherbourne (1994) used an FEM approach for the analysis of the 3D models, which suitably predicted the behavior of unstiffened, extended end-plate connections with four bolts. From these findings, they proposed new analytical formulas for the behavior prediction of connection components. They demonstrated that for an extended end-plate connection, the numerical results were comparable to the experimental ones.

Short thereafter, Borgsmiller (1995) proposed a simple design method for five specimens with extended, end-plate moment connections, along with four specimens with flush end-plate connections. However, they noted that when the end-plate reaches 90% of its ultimate strength, the effect of prying forces should be considered. Results revealed that if the applied loads are less than 90% of the end-plate's strength, then the end-plate could be considered as a thick plate and the prying forces effects can be ignored. However, when the applied loads exceeded that threshold, the

end-plate should be considered as thin, and the effect of prying forces must be completely considered.

More recently, Murray and Sumner (2003) proposed design methods for unstiffened and stiffened extended end-plates with four and eight bolts when subjected to seismic loading. Their proposed method was used as the design guideline in current study. Subsequently, Maggi *et al.* (2005) studied the behavior of two unstiffened end-plate moment connections with several bolts and end-plate thicknesses numerically and experimentally. The results demonstrated that failures associated with either formation of yield lines in the plates (Mode 1) or bolt tension failures (Mode 3) are well-defined, while failures due to combination of these mechanisms (Mode 2) represent a level of interaction between the end-plate and the bolts that is difficult to predict accurately.

Recently, Drosopoulos *et al.* (2012) studied the behavior of steel end-plate moment connections by finite element method of analysis, as well as experimentally to consider the impact of column stiffeners on the overall response, local buckling of the column, and friction of the beam to column interface. In the same year, Gorgun and Yilmaz (2012) proposed an analytical procedure to predict the behavior of the steel moment frames with semi-rigid joints, and in 2013 Gorgun (2013) proposed an analytical procedure to predict the behavior of the steel moment frames with flexible members. The linear and nonlinear analyses were applied for two planar steel structures. The method is readily implemented on a computer using matrix structural analysis techniques and is applicable for the nonlinear analysis of frameworks. Since then, Ghassemieh *et al.* (2014) in studying the influence of the axial force on the overall performance of the steel end-plate moment connection observed that the effect of the axial force on the end-plate connection can change the failure mode.

Despite widespread research on end-plate connections, only a few researchers have considered the flexibility of connections in studying the seismic behavior of structures. Specifically, Ang and Morris (1984) did this for steel frames with semi-rigid connections. The results showed that by appropriate modeling, connection stiffness could show the influence on the structural displacements and internal forces. Nader and Astaneh (1991) looked at fully-rigid, semi-rigid, and pinned connections under seismic loadings. The behavior of structures with pinned and semi-rigid connections under dynamic loading was studied, and their respective responses were compared to that of the rigid structure subjected to similar earthquakes. The results revealed a reduction in base shear in structure using pinned or semi-rigid connections. Additionally, Awkar and Lui (1999) studied the behavior of a five-story and eight-story frame with fully-rigid, semi-rigid, and pinned connections. Results demonstrated increased drift of the top stories and decreased base shear of the semi-rigid frames. The connection flexibility also caused the frame periods to spread over a wider spectrum, thereby increasing the importance of the higher mode contribution to structural response. More recently, Ghassemieh and Kiani (2013) investigated the seismic performance of reduced beam section frames (RBS) considering connection flexibility. The results highlighted the role of RBS on reducing the seismic demands in the panel zone.

Given the paucity of studies on the flexibility of beam to column connections, the study herein does so by considering extended end-plates. First, a connection that has been previously studied by Maggi *et al.* (2005) was used to verify the Abaqus based FEM approach used herein. After that verification, the proposed connections were modeled and the moment-rotation curves of the connections were obtained. Then, the connections were modeled in OpenSees (Mazzoni *et al.* 2005) using a bi-linear model. The model proposed by Lui and Lopes (1997) was used in a single story frame to verify the bilinear model in the dynamic analysis. By considering the flexibility of the connections, the real behavior of such connections in the steel moment frames is

investigated. Finally, the differences between the performance of fully-rigid connections and semi-rigid connections utilized in four, eight, and sixteen-story buildings are compared.

2. Connections classification

According to AISC (2010), connections are classified with respect to their strength, ductility, and initial stiffness.

Connections are classified as full strength or partial strength with respect to their plastic moment capacity. Connection strength is the largest moment that the connection can resist and is obtained from the moment-rotation curve. If there is no clear maximum point in the moment-rotation curve, the moment corresponding to the rotation of 0.02 rad is considered as the strength of the connection.

Connection ductility relates to the ability to resist inelastic rotations without a noticeable decrease in strength and is classified as either brittle or ductile. The threshold between brittle and ductile behavior is 0.03 rad, as specified in the AISC (2010) code.

Also, regarding stiffness classification, the initial stiffness parameter of a connection (m_{Ki}) is described as fully-rigid, semi-rigid, or pinned as defined as follows

$$m_{Ki} = \frac{K_i}{\left(\frac{EI}{L}\right)_{beam}} \quad (1)$$

in which, K_i , EI and L are the initial connection stiffness, the bending rigidity, and beam length beam, respectively. The connection is considered as rigid, if $m_{Ki} > 20$. It is classified as semi-rigid, if $2 < m_{Ki} < 20$ or as pinned, if $m_{Ki} < 2$.

3. Model buildings

Three steel frame models, as proposed by Jin and El-Tail (2005), including four, eight, and sixteen-story structural frames with identical floor plans were used to investigate the effect of connection flexibility. These and the elevations of the frames are depicted in Fig. 3.

In design of the three buildings, external frames resist lateral seismic loadings, and middle frames resist gravity loads. Distributed loads calculated for roof and the various stories are provided in Table 1.

The design base shear is determined following the provisions in chapter 5 of FEMA 302 (1997) as follow

$$V = C_s \cdot W \quad (2)$$

where W is the effective seismic weight consisting of dead loads plus 20% of the live loads, and C_s is the coefficient of seismic response of the structure. The values for W , C_s and V for the three frames are provided in Table 2.

Due to symmetry in two directions, only one direction was modeled. Also, the beam to column connections of the internal frames were assumed to be pinned (Jin and El-Tail 2005). Therefore, only the external frames resist the lateral loads. P-delta effects were also considered in the

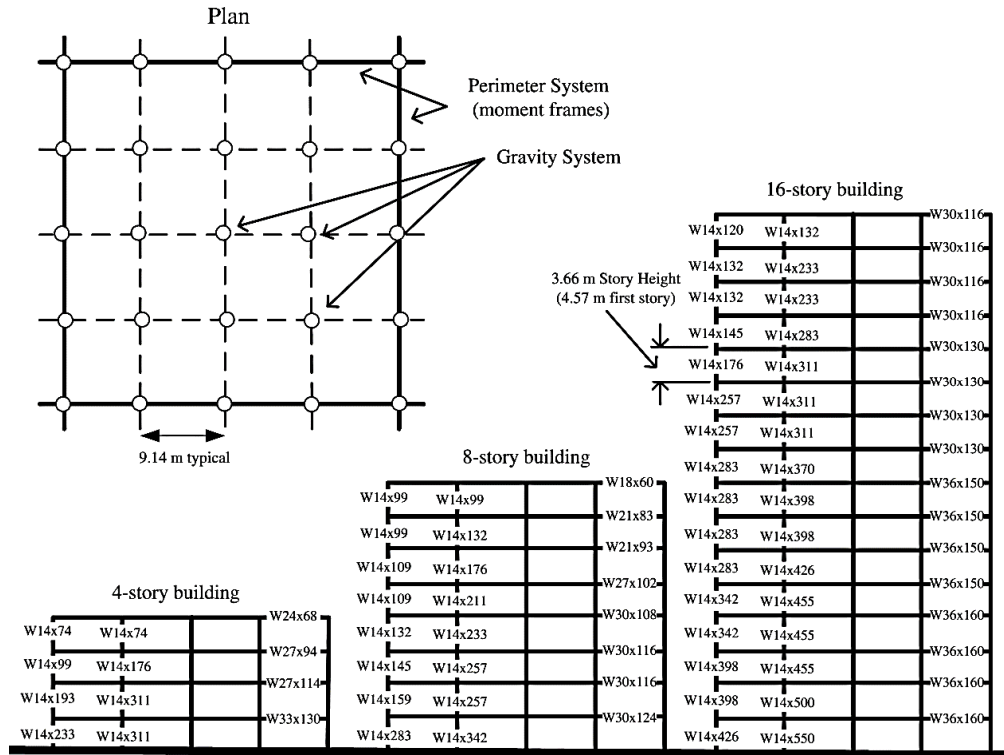


Fig. 3 Plan and elevation view of selected frames (Jin and El-Tail 2005)

Table 1 Story load distribution (Jin and El-Tail 2005)

	Dead load (Pa)	Live load (Pa)
Floors	5000	2400
Roof	3600	960

Table 2 Design shear force (Jin and El-Tail 2005)

Number of stories	4	8	16
W (kN)	27042	56341	114939
C_s	0.165	0.1	0.088
V (kN)	4462	5634	10114

analyses. All the connections for the above mentioned frames were designed in accordance with the design steps of the prequalified connections in AISC being the ANSI/AISC 358-05 (2005) standard, which follows the AISC design guide series 4 (Murray and Sumner 2003). Details of the designed connections are provided in Table 3. Fig. 4 and Table 4 provide the information on the geometrical details of the end-plate for the designed connections. The locations of the connections in the frames are presented in Table 5.

Table 3 Dimensions and characteristics of the connections

Connection	Column	Beam	Doubler plate thickness (mm)	Continuity plate thickness (mm)	d_{bolt} (mm)
BEC1	W14 × 233	W33 × 130	-	21.8	38
BEC2	W14 × 193	W27 × 114	6.8	23.6	38
BEC3	W14 × 99	W27 × 94	18	19	38
BEC4	W14 × 74	W24 × 68	12	15	32
BEC5	W14 × 283	W30 × 124	-	23.6	38
BEC6	W14 × 159	W30 × 116	14	21.6	38
BEC7	W14 × 132	W30 × 108	16	19.4	38
BEC8	W14 × 109	W27 × 102	19	21.2	38
BEC9	W14 × 109	W21 × 93	16.5	23.6	32
BEC10	W14 × 426	W36 × 160	-	26	38
BEC11	W14 × 398	W36 × 160	-	26	38
BEC12	W14 × 283	W36 × 150	-	24	38
BEC13	W14 × 257	W33 × 130	-	22	38
BEC14	W14 × 132	W30 × 116	18.2	21.6	38

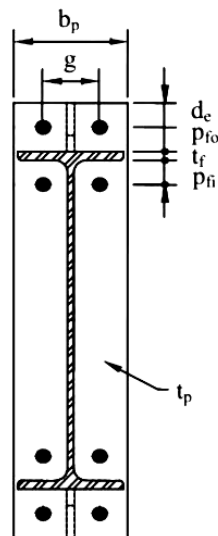


Fig. 4 End-plate geometric dimensions

Before modeling the proposed connections in Abaqus (2003), the appropriateness of the modeling approach was verified by modeling specimen CT1A-1, as tested by Maggi *et al.* (2005). In that, eight-node elements with three independent degrees of freedom for each node were used without reduction in the number of Gauss integration points (C3D8). Meshing details of the connection are shown in Fig. 5.

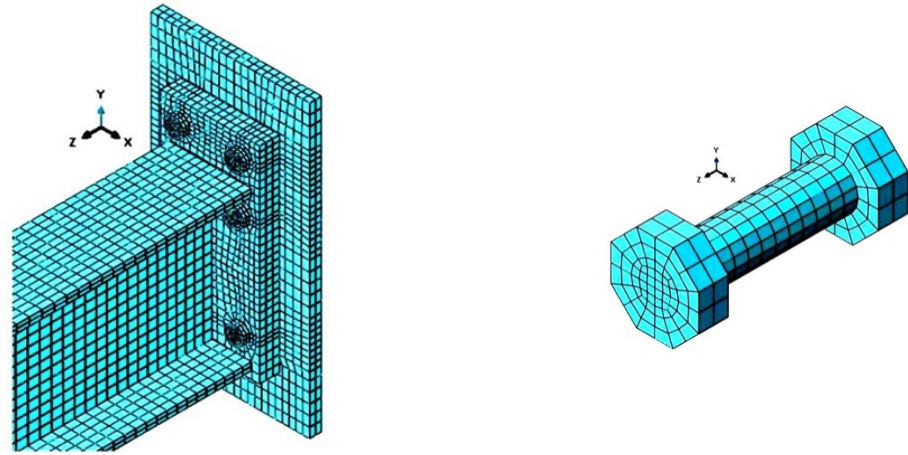
Table 4 Dimensions of the end-plate (mm)

Connection	b_p	t_p	g	d_e	$P_{fi} = p_{fo}$
BEC1	320	40	140	42	52
BEC2	280	40	140	42	52
BEC3	280	38	140	42	52
BEC4	254	32	140	42	52
BEC5	290	40	140	42	52
BEC6	290	40	140	42	52
BEC7	290	38	140	42	52
BEC8	280	38	140	42	52
BEC9	240	30	140	42	52
BEC10	330	40	190	42	52
BEC11	330	40	190	42	52
BEC12	330	38	140	42	52
BEC13	320	40	140	42	52
BEC14	290	40	140	42	52

Table 5 Location of the connections in the frames

Connection	Frame	Number of story
BEC1	4 story	1
BEC2	4 story	2
BEC3	4 story	3
BEC4	4 story	4
BEC5	8 story	1
BEC6	8 story	2 and 3
BEC7	8 story	4
BEC8	8 story	5
BEC9	8 story	6, 7 and 8
BEC10	16 story	1 and 2
BEC11	16 story	3 and 4
BEC12	16 story	5, 6, 7 and 8
BEC13	16 story	9, 10, 11 and 12
BEC14	16 story	13, 14, 15 and 16

Beams and columns used in the models were VS 250×37 and CVS 350×105 , respectively. Details of the end-plate proposed by Maggi *et al.* (2005) are illustrated in Fig. 6. A tri-linear, stress-strain relationship was utilized according to Sumner (2003). The stress-strain relationship utilized for the beam, end-plate and column flange steel is shown in Fig. 7(a). A yield strength of 288 MPa and an ultimate strength of 432 MPa were utilized. The selected high-strength bolt



(a) Overall view (along each thickness applied at least two rows of mesh)

(b) Bolts view

Fig. 5 Typical meshing pattern for 3D finite element model

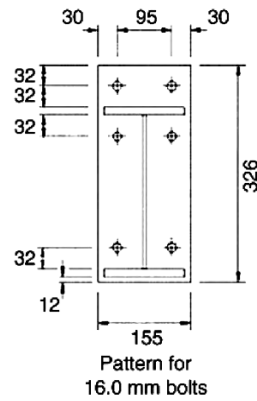
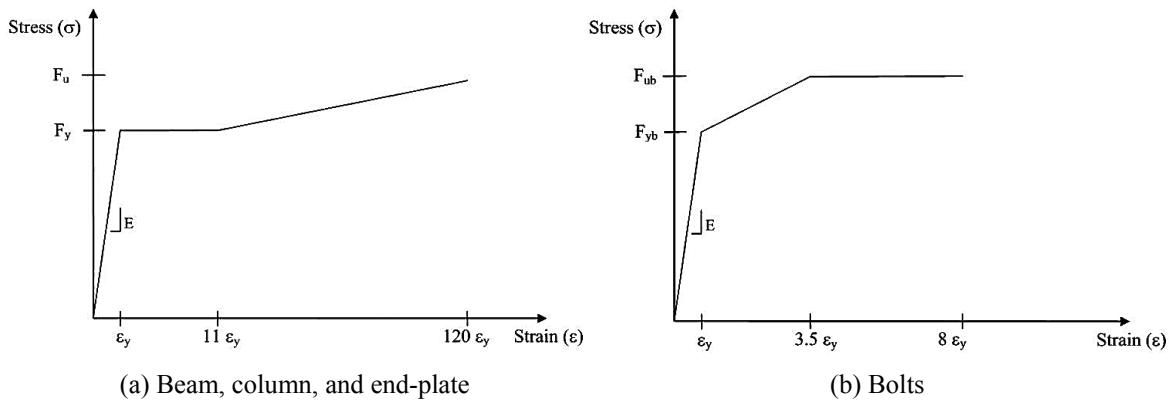


Fig. 6 End-plate details (Maggi *et al.* 2005)



(a) Beam, column, and end-plate

(b) Bolts

Fig. 7 Stress-strain diagrams for the components (Sumner 2003)

stress-strain relationship is shown in Fig. 7(b). The bolts have a diameter of 16 mm and are made of ASTM A325 steel with a yield stress of 635 MPa and an ultimate strength of 712 MPa. The modulus of elasticity of 2×10^5 MPa and the Poisson ratio of 0.3 were used in the analyses.

Since the column's web was not modeled, its deformation was ignored to simplify the modeling. Therefore, the displacement degrees of freedom of the nodes located in column's web, along with the nodes located between the continuity plates and column's flange were considered to be restrained. The friction coefficient (μ_s) was considered to be 0.3 for all contact surfaces. Fig. 8 shows the boundary conditions of the model.

The loading procedure consisted of two stages including the pre-tensioning of the bolts by applying negative temperature to each bolt shank and then by applying deformation to the end of the beam until the connection collapsed. Subsequently, the moment-rotation curve of the

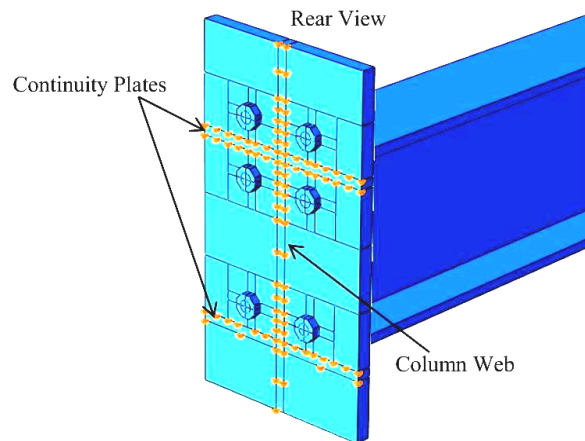


Fig. 8 Boundary conditions of the connection

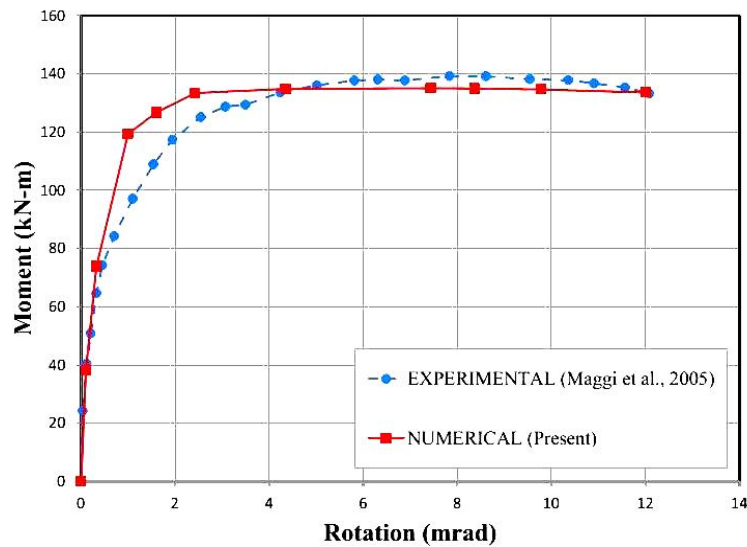


Fig. 9 Moment-rotation curve of the specimen

benchmark model resulting from the FEM analysis was obtained and compared with that of the experimental test, as illustrated in Fig. 9. Rotation of the connection was calculated as the ratio of the separation distance of the end-plate and the tensile flange of the beam to the distance between the beam flanges.

The ultimate moment capacity resulting from the finite element analysis was 133.6 kN.m, which coincided closely with the experimental result of 136 kN.m. The end-plate relative displacements for the two cases of the finite element analysis and the experimental test for $M = 117$ kN.m are illustrated in Fig. 10.

As shown, the results from the finite element analysis show good correlation with the experimental results, except for the rotations between 1 and 2 mrad. This discrepancy is attributed to the fact that some bolts lost their pretension forces in the assemblage sequence during the experimental program (Maggi *et al.* 2005). Nevertheless, the overall predicted bending resistance of the model matched very well with the experimental test. Also, the experimental results for CT1A-1 showed that the connections failed as a result of bolt failures in the tension zone, which is consistent with the predictions of the finite element models.

For the modeling of the extended end-plates, the exterior beam to column connections were

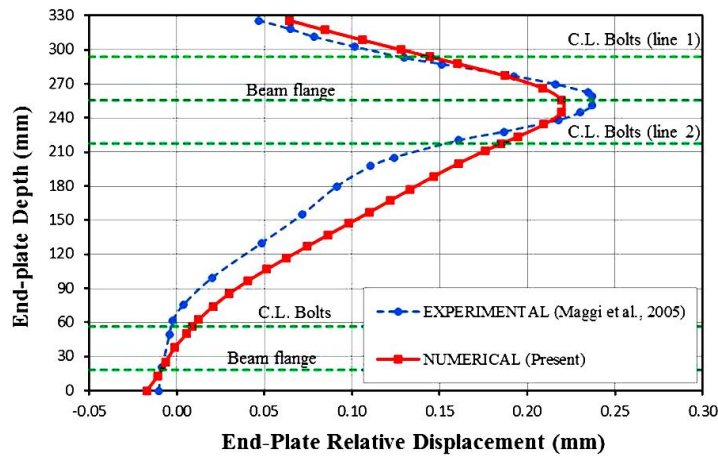


Fig. 10 End-plate separation

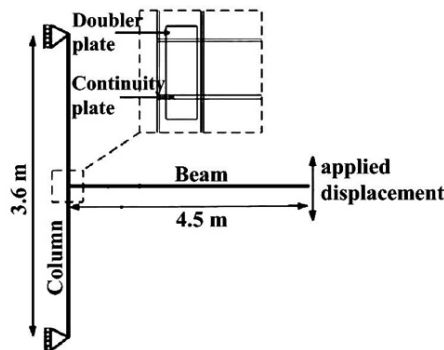


Fig. 11 Frames' exterior connections modeling

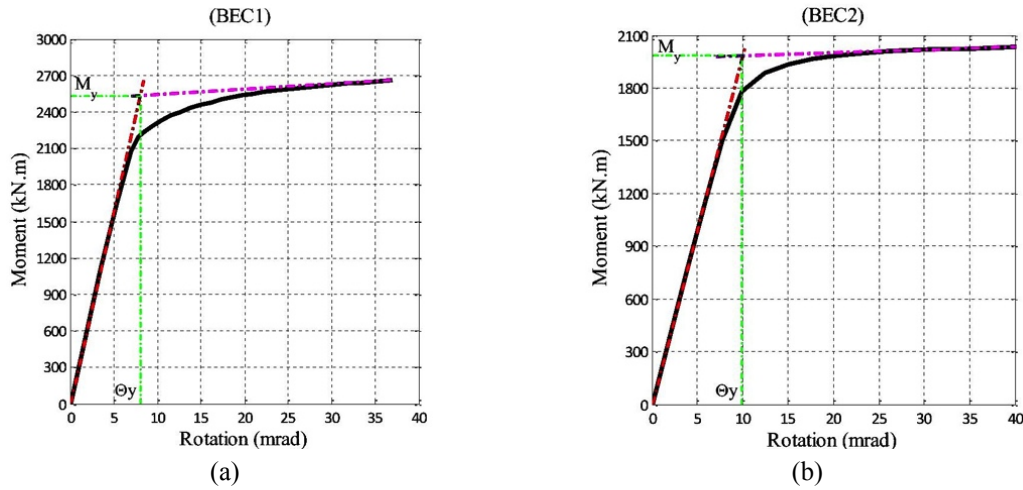


Fig. 12 Moment-rotation curves for BEC1 and BEC2

used for the modeling (Fig. 11), and the appropriate restraints at the ends of the columns were used in Abaqus (2003) in order to ensure pinned support condition. The steel for the beams, columns and end-plates had yield and ultimate strengths of 345 MPa and 460 MPa, respectively. Bolts were made according to ASTM A490 with yield and ultimate strengths of 779 MPa and 1,035 MPa, respectively. The constitutive models of the materials were the same as those in Fig. 7. Connection rotation was obtained through the calculation of the difference between rotation of the beam and the column.

Moment-rotation curves for the connections BEC1 and BEC2 are illustrated in Fig. 12 in which M_y is the connection's yield moment obtained from the intersection of the initial and second slopes (Mohamadi-Shoore and Mofid 2011, Sumner 2003).

The results from FEM analyses emphasize that after the beam flange buckling occurs, the main failure is mode 2 – formation of a plastic hinge at the beam web followed by yielding of the bolt. This is in consistent with the AISC design guide series 4 (Murray and Sumner 2003). As expected the location of the plastic hinges in most connections was detected in the beam at the one-half depth distance from the face of the end-plate. Connection categories are shown in Table 6.

Bi-linear modeling was used for moment-rotation curves of the connections and had three parameters including elastic stiffness of the connection (K_i), secondary stiffness (K_p), and yield moment M_y as depicted in Fig. 13.

A Nonlinear Beam Column Element was used for the modeling of beams and columns. This is based on the force formulation and considers the spread of plasticity along the element. In this element, the plasticity is distributed over the element's entire length.

The arguments to construct the element are its tag, the two end nodes, the number of integration points along the element, the section tag, and the geometric transformation tag. The integration along the element is based on the Gauss-Lobatto quadrature rule (two integration points at the element ends). The element is prismatic. An element mass density per unit length, from which a lumped mass matrix is formed, is specified. The arguments for the iterative form are the maximum number of iterations to undertake to satisfy element compatibility and the tolerance for satisfaction of element compatibility.

Table 6 Categories of the connections

Connection	K_i (kN.m/rad)	m_{K_i}	Category
BEC1	314,730	5.07	Semi-Rigid
BEC2	199,178	5.26	Semi-Rigid
BEC3	155,723	5.14	Semi-Rigid
BEC4	89,441	5.28	Semi-Rigid
BEC5	260,861	5.26	Semi-Rigid
BEC6	238,187	5.22	Semi-Rigid
BEC7	211,538	5.11	Semi-Rigid
BEC8	171,950	5.13	Semi-Rigid
BEC9	101,149	5.28	Semi-Rigid
BEC10	517,692	5.74	Semi-Rigid
BEC11	458,211	5.08	Semi-Rigid
BEC12	421,271	5.03	Semi-Rigid
BEC13	317,244	5.11	Semi-Rigid
BEC14	235,716	5.16	Semi-Rigid

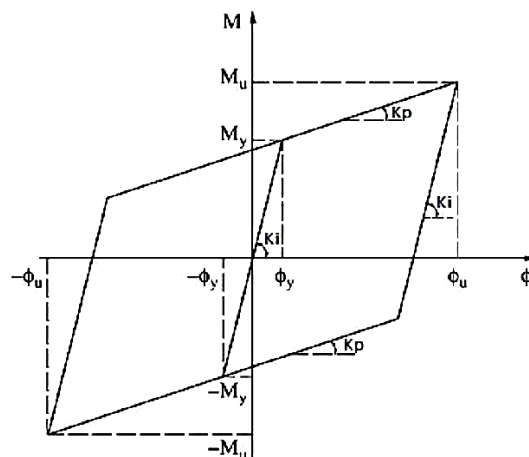


Fig. 13 Bilinear modeling of the connections

The axial and flexural responses of each plastic hinge region are defined as separate sections. The axial response is defined by an elastic section, while the flexural response is defined by a uniaxial section. The overall responses are combined into a single section. The element Zerolength in OpenSees (Mazzoni *et al.* 2005) was selected as a spring element to define the moment-rotation curvature between the beam-column joint nodes. Also, Steel01 was chosen to employ the bi-linear behavior of steel, as shown in Fig. 14 in which, F_y , $E0$ and b are yield strength, the initial elastic tangent, and strain-hardening ratio, respectively. Stiffness characteristics of the designed connections for 2D simulation in OpenSees (Mazzoni *et al.* 2005) are outlined in Table 7. Also, to model the frames with fully-rigid joints, the rotational springs with infinite initial stiffness were utilized in the connection joints.

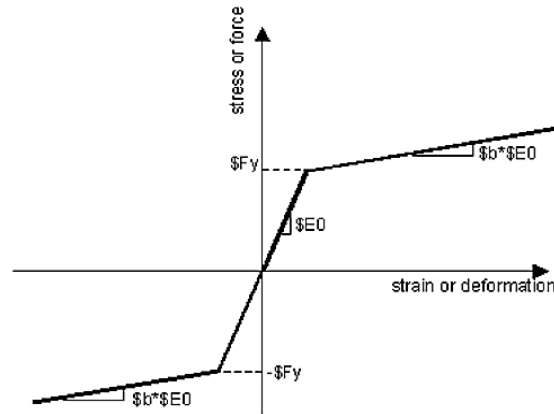
Fig. 14 Steel01 material in OpenSees (Mazzoni *et al.* 2005)

Table 7 2D characteristics of the connections

Connection	$E0$ (kN.m/rad)	F_y (kN.m)	b
BEC1	314,730	2531	0.0139
BEC2	199,178	1982	0.0086
BEC3	155,723	1598	0.0081
BEC4	89,441	1022	0.0083
BEC5	260,861	2356	0.0089
BEC6	238,187	2211	0.0077
BEC7	211,538	1986	0.0092
BEC8	171,950	1760	0.0083
BEC9	101,149	1269	0.0091
BEC10	517,692	2945	0.0525
BEC11	458,211	3132	0.0210
BEC12	421,271	2978	0.0225
BEC13	317,244	2558	0.0232
BEC14	235,716	2185	0.0118

A one-story frame proposed by Lui and Lopes (1997) was used to verify the proposed 2D spring model in OpenSees. Then, the behavior of the frame with both rigid and semi-rigid connections were compared with that of the models proposed by Lui and Lopes (1997). The frame model, the material properties, and connections' parameters for the frame are shown in Fig. 15 and Table 8, respectively. Connection parameters for the frames with the extended end-plate connector, as well as with the rigid connections are outlined in Table 9.

Table 10 presents the numerical results produced herein and the results reported by Lui and Lopes (1997) for the natural periods of the structure without axial loading on columns, and the structure with columns' axial force equal to $0.3P_y$ in which, P_y is the yielding axial force of the column. The results demonstrate that the proposed models can suitably predict the results of the tests.

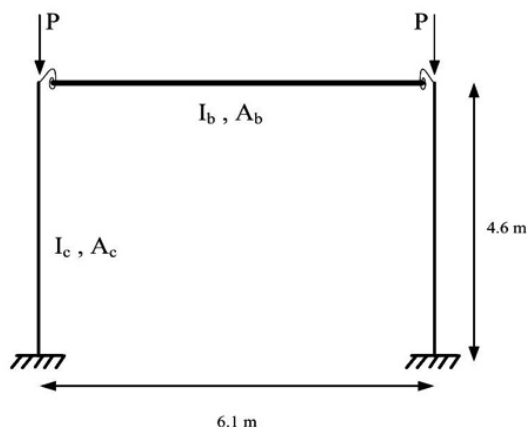


Fig. 15 Semi-rigid frame model (Lui and Lopes 1997)

Table 8 Members and material properties (Lui and Lopes 1997)

Member	E (MPa)	F_y (MPa)	L (m)	I (m ⁴)	A (m ²)
Beam	2.04×10^5	252.8	6.1	5.54×10^{-4}	0.0120
column	2.04×10^5	252.8	4.6	1.13×10^{-4}	0.0093

Table 9 Connections' parameters (Lui and Lopes 1997)

Connection	K_i (kN.m/rad)	K_p (kN.m/rad)	M_y (kN.m)
Extended end-plate	34000	2260	170
Rigid	∞	∞	–

Table 10 Comparison of change in natural periods, T_n (s)

Connection	T_n ($P/P_y = 0$)		T_n ($P/P_y = 0.3$)	
	Present study	Lui and Lopes 1997	Present study	Lui and Lopes 1997
Extended end-plate	0.096	0.096	0.100	0.100
Rigid	0.084	0.084	0.087	0.087

Also, Lui and Lopes (1997), did some forced vibration analysis. The harmonic loading given by Eq. (3) was applied to the roof to calculate the normalized dynamic response, (R_d), of the structure in the two cases of the connection with extended end-plates, and rigid connections. This was done so that the model could be verified against the work of Lui and Lopes (1997). Forced vibration analysis allows insight into semi-rigid frame performance in terms of maximum response characteristics, such as base shear attributes and energy dissipation capacity. These specifics are described below.

In Eq. (3), m is the system mass, ω is the frequency of the external load, and g is the gravitational acceleration.

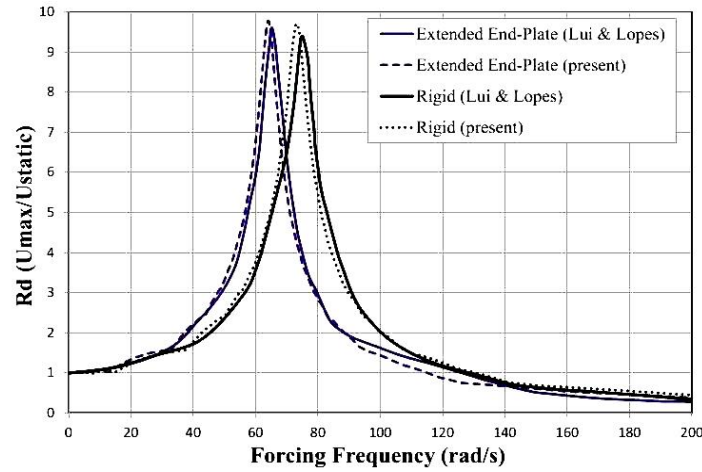


Fig. 16 Displacement response curves

$$F(t) = P_0 \sin(\omega t) = 0.2 \text{ mg} \sin(\omega t) \quad (3)$$

The normalized dynamic response (R_d) is obtained as follows

$$R_d = \frac{U_{dynamic}(\max)}{U_{static}(\max)} \quad (4)$$

in which, $U_{dynamic}(\max)$ is the maximum displacement in each frequency of the external load, and $U_{static}(\max)$ is the maximum displacement. The displacement response curves of the finite element model and tests by Lui and Lopes (1997) are presented in Fig. 16. This shows that the bi-linear model created in OpenSees provides suitable answers indicating that the model was accurately simulated.

4. Modal analysis

Using the modal analyses, the periods of the extended plate connectors were calculated as presented in Table 11. By enabling connection flexibility in the model, periods corresponding to the first modes are increased, whereas the effect on higher modes is insignificant.

5. Nonlinear static analysis (Pushover)

To investigate the behavior of the three, multi-story frames with pushover analysis, modal and triangular loading patterns were applied, as suggested by FEMA 356 (2000a). Due to the significant difference between the first and second period of the structure, the modal loading pattern corresponding to the first shape mode of the structure was used in the analysis. For the triangular loading pattern, the lateral load coefficient (C_x) was obtained with Eq. (5)

Table 11 Comparison of the frames' periods (s)

Mode No.	4-story		8-story		16-story	
	Fully-rigid	Semi-rigid	Fully-rigid	Semi-rigid	Fully-rigid	Semi-rigid
1	1.01	1.25	2.07	2.63	2.95	3.79
2	0.40	0.46	0.79	0.98	1.07	1.37
3	0.23	0.25	0.45	0.54	0.63	0.80
4	0.14	0.14	0.31	0.36	0.44	0.55
5			0.23	0.26	0.34	0.41
6			0.18	0.19	0.27	0.32
7					0.23	0.26
8					0.19	0.22
9					0.16	0.18

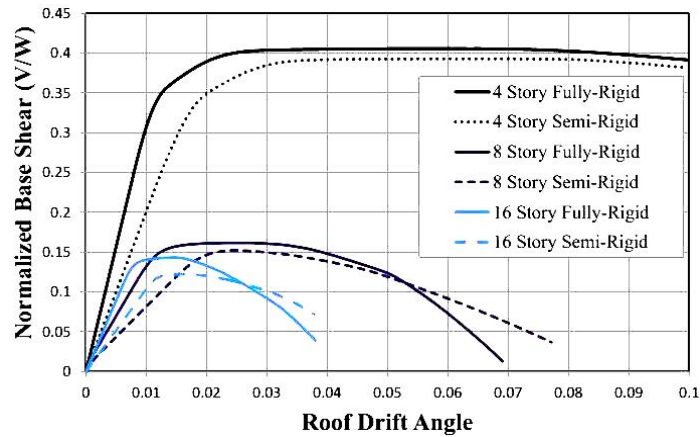


Fig. 17 Pushover response curves (modal loading pattern)

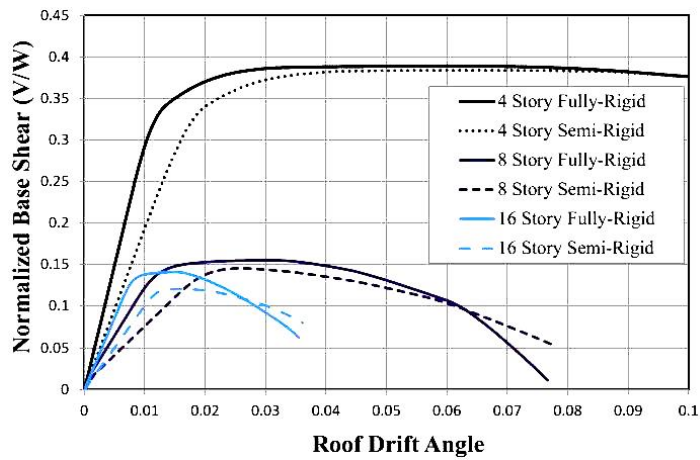


Fig. 18 Pushover response curves (triangular loading pattern)

$$C_x = \frac{W_x h_x^k}{\sum_{i=1}^n W_i h_i^k} \quad (5)$$

where W_i and h_i are the weight and height of the i th story, respectively. Also, k is a coefficient corresponding to the period of the structure and was taken as 1.35 for the 4-story and 2 for the 8- and 16-story buildings in this study. Overall, structural response (as a function of base shear versus roof drift angle under modal and triangular loadings) are depicted in Figs. 17 and 18, respectively. In these figures, base shear of the building is normalized with respect to the weight of the building, and the drift rotation is calculated as roof displacement over the total building height.

Figs. 17 and 18 show several important regions in the response curves including an elastic region, a transitional region with decreasing stiffness, a yielding plateau with almost zero stiffness, and a descending branch with negative stiffness. Inclusion of the beam to column connection flexibility results in stiffness reduction within the elastic range of all curves. In frames with semi-rigid connections, strength loss in the strength reduction zone is less severe than that for frames with fully-rigid connections. Moreover, frames with semi-rigid connections have longer yielding regions compared to the frames with fully-rigid connections. Furthermore, a comparison between response curves of the 4-, 8- and 16-story structures shows that with increasing building stories, P-Delta effects gain great importance, as the slope of the response curve of the structure in the strength degradation zone steepens.

According to the results from the non-linear static analyses, the over strength factors, defined as the ratio of the real strength over design strength, are listed for modal and triangular loading pattern in Tables 12 and 13. These ranged from a minimum of 1.61 to a maximum of 2.46. When the semi-rigid is compared to the rigid, the semi-rigid produced as little as 1.27% to more as much as 14.4%.

As seen, the over strength factor in frames with fully-rigid connections is larger than that in frames with semi-rigid connections, thereby implying that by considering the flexibility of the beam to column connection results in considerable strength degradation of the structure. With an increase in the number of stories, the difference between the values of over-strength factors in the two cases of rigid and semi-rigid becomes noticeable.

Table 12 Over strength factor level for modal loading pattern

Connection's type	4-Story	8-Story	16-Story
Fully-rigid	2.46	1.61	1.62
Semi-rigid	2.38	1.52	1.39
Difference (%)	3.25	5.59	14.19

Table 13 Over strength factor level for triangular loading pattern

Connection	4-Story	8-Story	16-Story
Fully-rigid	2.35	1.55	1.60
Semi-rigid	2.32	1.45	1.37
Difference (%)	1.27	6.45	14.4

6. Incremental dynamic analysis

Dynamic behavior of the three frames was investigated through the application of incremental dynamic analyses (IDA) involves performing multiple, nonlinear dynamic analyses of a structural model under a suite of ground motion records. Each is scaled to several levels of seismic intensity. The scaling levels are appropriately selected to force the structure through the entire range of behavior, from elastic to inelastic and finally to global dynamic instability, where the structure essentially experiences collapse (Vamvatsikos and Cornell 2002). To achieve this herein, 22 earthquake records were selected, as shown in Table 14.

IDA employs a number of non-linear dynamic analyses under some scaled earthquake records to predict seismic demand and capacity. The approach requires some parameters such as earthquake intensity measure (IM) and damage measure (DM). In this study, peak ground acceleration (PGA) and maximum inter-story drift angle (θ_{max}) were considered as the IM and DM, respectively.

According to FEMA 350 (2000b), the two performance levels of immediate occupancy (IO) and collapse prevention (CP) were selected so as to compare the three frames for the two cases of fully-rigid and semi-rigid connections. As stated in FEMA 350 (2000b), the maximum allowable

Table 14 Details of the selected ground motions

Name	Ground motion name	Station	PGA (g)
1	Imperial Valley 1979	Chihuahua	0.254
2	Imperial Valley 1979	Chihuahua	0.27
3	San Fernando 1971	Hollywood Stor Lot	0.21
4	Superstitt Hills (A) 1987	Wildlife Liquefaction Array	0.132
5	Superstitt Hills (A) 1987	Wildlife Liquefaction Array	0.134
6	Superstitt Hills (B) 1987	Plaster City	0.186
7	Landers 1992	Barstow	0.135
8	Cape Mendocino 1992	Rio Dell Overpass	0.385
9	Coalinga 1983	Parkfield-Fault Zone 3	0.164
10	Imperial Valley 1979	El Centro Array #12	0.143
11	Loma Prieta 1989	Anderson Dam Downstream	0.244
12	Loma Prieta 1989	Agnews State Hospital	0.159
13	Loma Prieta 1989	Anderson Dam Downstream	0.244
14	Loma Prieta 1989	Coyote Lake Dam Downstream	0.179
15	Imperial Valley 1979	Cucapah	0.309
16	Loma Prieta 1989	Sunnyvale Colton Ave	0.207
17	Imperial Valley 1979	El Centro Array #13	0.117
18	Imperial Valley 1979	Westmoreland Fire Station	0.074
19	Loma Prieta 1989	Sunnyvale Colton Ave	0.209
20	Imperial Valley 1979	El Centro Array #13	0.139
21	Imperial Valley 1979	Westmoreland Fire Station	0.11
22	Loma Prieta 1989	Hollister Diff. Array	0.269

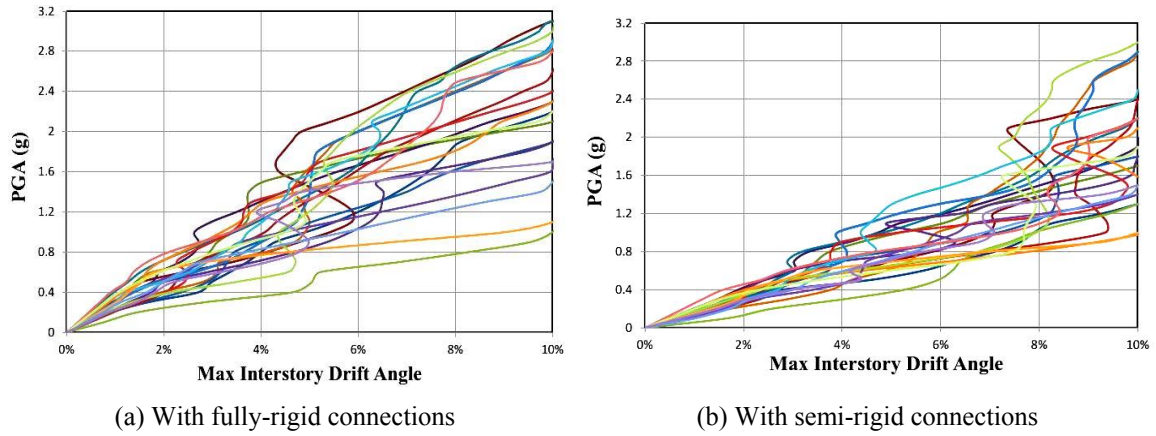


Fig. 19 Full IDA curves for the four-story frame

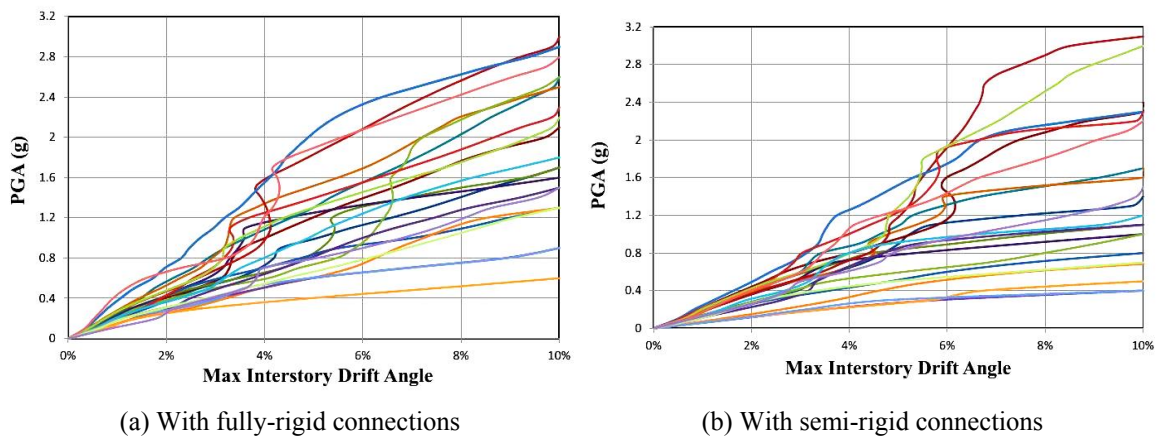


Fig. 20 Full IDA curves for the eight-story frame

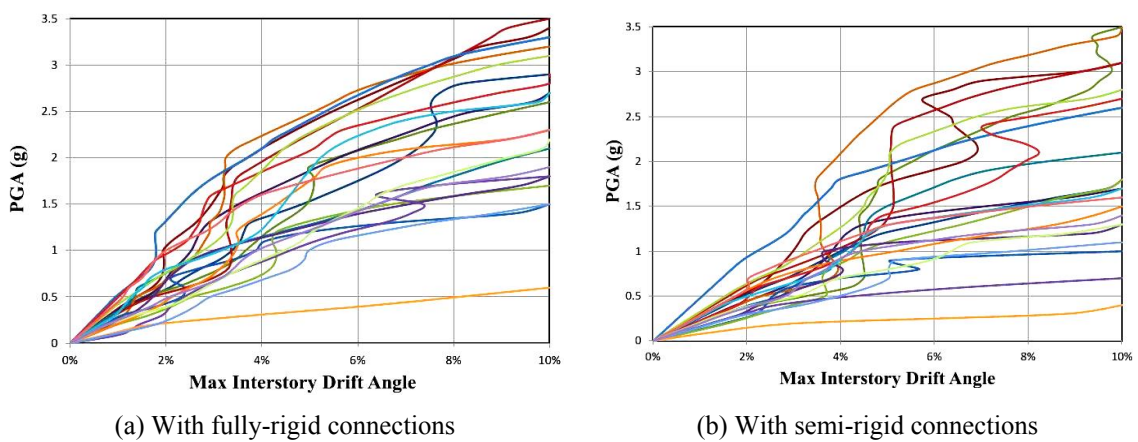


Fig. 21 Full IDA curves for the sixteen-story framed

rotation for IO and CP levels are 2% and 10%, respectively. For data categorization, a multi-IDA curve is obtained. For this study, the mean minus two times the standard deviation (16% of the data), the average of the data (50% of data), and 2 times the standard deviation (84% of the data) were used. All 3 structures were analyzed with both the fully-rigid and semi-rigid conditions using IDA with the 22 records; each with 35 (per 0.1 g) scaled coefficients. Thus, a total of 4,620 time history analyses were performed. In this study, the maximum inter-story drift angle was chosen as the controlling criterion for the response of the structure. The θ_{max} -PGA curves were obtained from the IDA under the selected records of the three frames as depicted in Figs. 19-21.

As observed in Figs. 19-21, for most PGAs, the maximum inter-story drifts of frames with semi-rigid connections are higher than for frames with fully-rigid connections. These figures were used to extract the multi-IDA curves as shown in Figs. 22-24.

As seen in Fig. 22, for the four-story frame, the difference between the required PGA to pass the IO level for the fully-rigid connections is 32.5%, 36.5%, and 38.4% versus 16%, 50%, and 84% for the semi-rigid connection. But for CP level, the difference between the two cases is

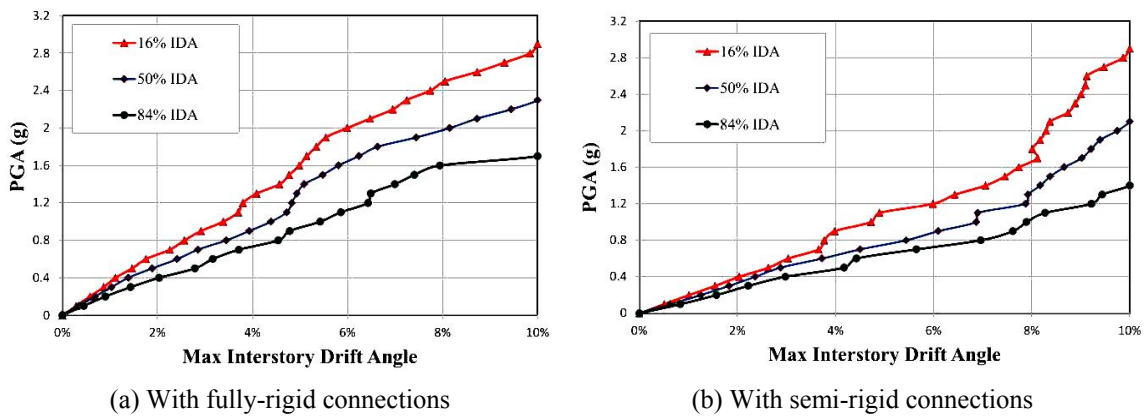


Fig. 22 Multi-IDA curves for the four-story frame

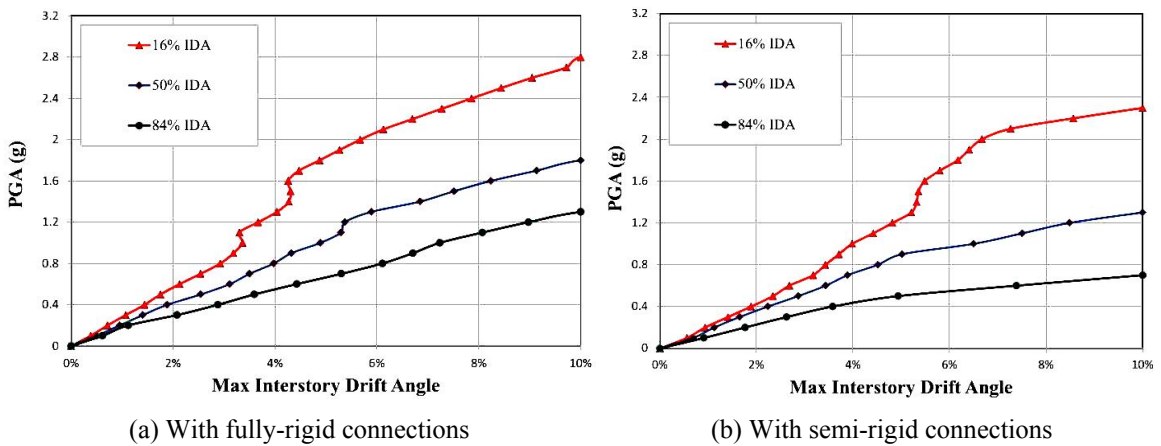


Fig. 23 Multi-IDA curves for the eight-story frame

negligible. Likewise, as illustrated in Figs. 23 and 24, for the 8- and 16-story frames, the difference between the required PGA to pass IO level is high. However, for the CP level, the difference between the required PGA for the two cases of fully-rigid and semi-rigid connection

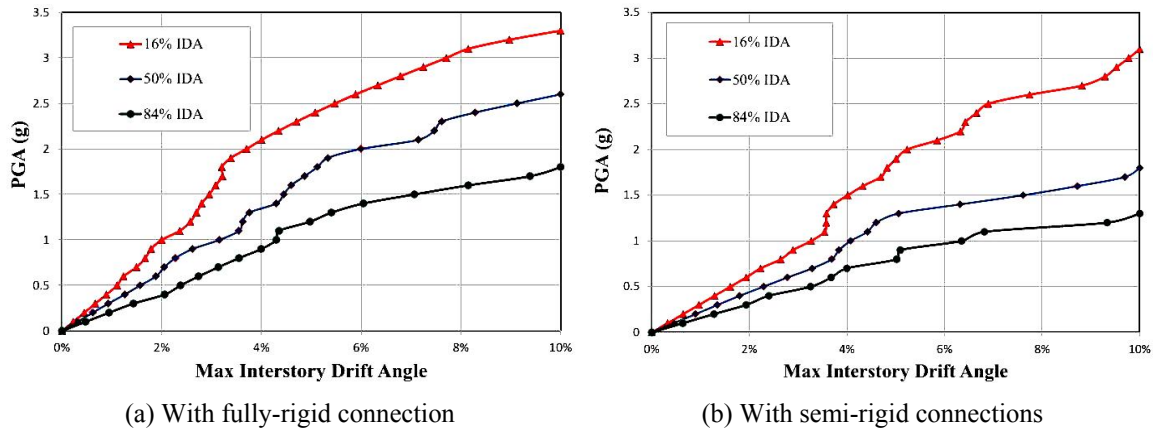


Fig. 24 Multi-IDA curves for the sixteen-story frame

Table 15 Minimum PGAs (g) required to pass defined performance levels for the four-story frame

	IO			CP		
	Fully-rigid	Semi-rigid	Difference (%)	Fully-rigid	Semi-rigid	Difference (%)
16% of data	0.4	0.27	32.5	1.7	1.4	17.6
50% of data	0.52	0.33	36.5	2.3	2.1	8.7
84% of data	0.65	0.4	38.4	2.9	2.9	0

Table 16 Minimum PGAs (g) required to pass defined performance levels for the eight-story frame

	IO			CP		
	Fully-Rigid	Semi-Rigid	Difference (%)	Fully-Rigid	Semi-Rigid	Difference (%)
16% of data	0.28	0.23	17.8	1.3	0.7	46.1
50% of data	0.42	0.36	14.3	1.8	1.3	27.7
84% of data	0.57	0.42	26.3	2.8	2.3	17.8

Table 17 Minimum PGAs (g) required to pass defined performance levels for the sixteen-story frame

	IO			CP		
	Fully-rigid	Semi-rigid	Difference (%)	Fully-rigid	Semi-rigid	Difference (%)
16% of data	0.38	0.31	18.4	1.8	1.3	27.7
50% of data	0.67	0.45	32.8	2.6	1.8	30.7
84% of data	1	0.62	38	3.3	3.1	6

decreased. This means that the behavior of frames with fully-rigid and semi-rigid connection under low PGAs versus high PGAs is completely different. Tables 15-17 present the minimum PGAs required to pass the defined performance levels for the 4-, 8-, and 16-story frames, respectively.

As shown, there is a significant difference between the two cases of fully-rigid and semi-rigid frames in terms of the minimum PGA required to pass the defined performance levels. For the frames with connections modeled as fully-rigid, the results of the dynamic analyses indicate that such an assumption produces non-conservative results.

7. Conclusions

The goal of the current research was to investigate the performance of the frames with extended end-plate moment connections by explicitly considering their flexibility. To determine the behavior, the connection was investigated using finite element analysis. Then, the behavior of the frames was studied through incremental and multiple dynamic analysis. The major findings were as follows:

- Having obtained the stiffness of the connections, it was revealed that all connections behave as semi-rigid in accordance with AISC (2010) connection classifications (see Table 6).
- Inclusion of connection flexibility reduced the frame strength (Tables 12 and 13) and stiffness (Figs. 17 and 18) but increased the natural period (Table 11).
- Frames with semi-rigid connections experienced larger maximum inter-story drifts than frames with fully-rigid connections under a constant PGA of a specified record.
- For the 4-, 8-, and 16--story frames, the difference between PGAs for the fully-rigid versus the semi-rigid connections for 84% of data at the CP level was negligible.
- The impact of considering the relative connection flexibility has a much more severe implication for smaller structures, with respect to the immediate occupancy, than for taller structures (Tables 15-17).

References

- Abaqus User's Manual (2003), Version 6.4, Abaqus Inc., Providence, R.I.
- AISC (1989), Specification for Structural Steel Buildings, Chicago, IL, USA.
- AISC (2010), Specification for Structural Steel Buildings, Chicago, IL, USA.
- Ang, K.M. and Morris, G.A. (1984), "Analysis of three-dimensional frames with flexible beam-column connections", *Can. J. Civil Eng.*, **11**(2), 245-254.
- ANSI/AISC 358-05 (2005), Prequalified connections for special and intermediate steel moment frames for seismic applications; American Institute of Steel Construction, Chicago, IL, USA.
- Awkar, J.C. and Lui, E.M. (1999), "Seismic analysis and response of multistory semirigid frames", *Eng. Struct.*, **21**(5), 425-441.
- Bahaari, M.R. and Sherbourne, A.N. (1994), "Computer modelling of an extended endplate bolted connection", *Comput. Struct.*, **52**(5), 879-893.
- Borgsmiller, J.T. (1995), "Simplified method for design of moment endplate connections", M.S. Thesis; Department of Civil Engineering, Virginia Polytechnic Institute and State University, Blacksburg, VA, USA.
- Drosopoulos, G.A., Stavroulakis, G.E. and Abdalla, K.M. (2012), "3D finite element analysis of end-plate steel joints", *Steel Compos. Struct., Int. J.*, **12**(2), 93-115.

- FEMA (1997), FEMA-302 — NEHRP recommended provisions for seismic regulations for new buildings; Federal Emergency Management Agency, Washington, D.C., USA.
- FEMA (2000a), FEMA-356 — Rehabilitation of buildings, prepared by ASCE for federal Emergency Management Agency (Prepared by ASCE); Federal Emergency Management Agency, Washington, D.C., USA.
- FEMA (2000b), FEMA-350 — Recommended seismic design criteria for new steel moment-frame buildings (prepared by SAC joint venture); Federal Emergency Management Agency, Washington, D.C., USA.
- Ghassemieh, M. and Kiani, J. (2013), “Seismic evaluation of reduced beam section frames considering connection flexibility”, *Struct. Des. Tall Spec. Build.*, **22**(16), 1248-1269.
- Ghassemieh, M., Kukreti, A.R. and Murray, T.M. (1983), “Inelastic finite element analysis of stiffened endplate moment connections”, Research Report No. FSEL/MBMA 83-02; Fears Structural Engineering Laboratory, School of Civil Engineering and Environmental Science, University of Oklahoma, Norman, OK, USA.
- Ghassemieh, M., Shamim, I. and Gholampour, A.A. (2014), “Influence of the axial force on the behavior of endplate moment connections”, *Struct. Eng. Mech., Int. J.*, **49**(1), 23-40.
- Gorgun, H. (2013), “Geometrically nonlinear analysis of plane frames composed of flexibly connected members”, *Struct. Eng. Mech., Int. J.*, **45**(3), 277-309.
- Gorgun, H. and Yilmaz, S. (2012), “Geometrically nonlinear analysis of plane frames with semi-rigid connections accounting for shear deformations”, *Struct. Eng. Mech., Int. J.*, **44**(4), 539-569.
- Jin, J. and El-Tawil, S. (2005), “Seismic performance of steel frames with reduced beam section connections”, *J. Construct. Steel Res.*, **61**(4), 453-471.
- Kukreti, A.R., Murray, T.M. and Ghassemieh, M. (1990), “Behavior and design of large capacity moment end-plates”, *Struct. Eng., ASCE*, **116**(3), 809-828.
- Lui, E.M. and Lopes, A. (1997), “Dynamic analysis and response of semi rigid frames”, *Eng. Struct.*, **19**(8), 644-654.
- Maggi, Y.I., Goncalves, R.M., Leon, R.T. and Ribeiro, L.F.L. (2005), “Parametric analysis of steel bolted end-plate connections using finite element modeling”, *J. Construct. Steel Res.*, **61**(5), 689-708.
- Mazzoni, S., McKenna, F. and Fenves, G.L. (2005), OpenSees command language manual; Pacific Earthquake Engineering Research (PEER) Center.
- Mohamadi-Shooreh, M.R. and Mofid, M. (2011), “New modeling for moment-rotation behavior of bolted endplate connections”, *Scientia Iranica*, **18**(4), 827-834.
- Murray, T.M. and Kukreti, A.R. (1988), “Design of 8-bolt stiffened moment end-plates”, *Eng J., AISC*, **25**(2), 45-52.
- Murray, T.M. and Sumner, E.A. (2003), AISC design guide series 4 (extended end-plate moment connections); American Institute of Steel Construction, Chicago, IL, USA.
- Nader, M.N. and Astaneh, A. (1991), “Dynamic behavior of flexible, semirigid and rigid steel frames”, *J. Construct. Steel Res.*, **18**(3), 179-192.
- Popov, E.P. and Tsai, K.C. (1989), “Performance of large seismic steel moment connections under cyclic loads”, *Eng. J.*, **26**(2), 51-60.
- Sumner, E.A. (2003), “Unified design of extended end-plate moment connections subject to cyclic loading”, Ph.D. Dissertation; Department of Civil Engineering, Virginia Polytechnic Institute and State University, Blacksburg, VA, USA.
- Tsai, K. and Popov, E. (1990), “Cyclic behavior of end-plate moment connections”, *J. Struct. Eng.*, **116**(11), 2917-2930.
- Vamvatsikos, D. and Cornell, C.A. (2002), “Incremental dynamic analysis”, *Earthq. Eng. Struct. Dyn.*, **31**(3), 491-514.